35th Annual International Conference of the IEEE EMBS
Osaka, Japan, 3 - 7 July, 2013

A Novel Method for Monolithic Fabrication of Polymer Microneedles on a Platform for Transdermal Drug Delivery

Buddhadev P. Chaudhuri, F. Ceyssens, C. Van Hoof, and R. Puers

Abstract— **This paper reports on the creation of a novel method for monolithic fabrication of out-of-plane polymer (SU-8) microneedles incorporating sharpness of needle-tips, hollowness of needle lumen as well as a platform on which the microneedles stand orthogonally with the hollow of the needle lumen continuous through the platform. In essence, both the microneedle as well as the platform on which it stands, are made of the same polymer material, rendering the process monolithic. The microneedle tips produced were quite sharp with tip diameters ranging between 5 to 10 µm, needle heights greater than 1 mm and resulting aspect ratio of 40. Further, mechanical tests performed on the fabricated microneedles demonstrate a critical compressive failure load of about 173 mN on average per microneedle, which translates into a safety factor greater than one for skin penetration.**

I. Introduction

Oral administration of drugs is one of the oldest methods of drug delivery prevalent even till date. When ingested orally, the drug is absorbed from the gastro-intestinal (GI) tract and is transported via the portal vein to the liver which metabolizes some of the drug. This phenomenon is called the first-pass metabolism effect and is the main reason why the drug entering the systemic circulation after this process, is of much reduced concentration and therefore has a low bioavailability. Bioavailability is the fraction of a drug that enters the systemic circulation after being administered via a certain route. This is the primary disadvantage of the oral route of drug delivery, namely, the incomplete metabolism and first-pass metabolism reduce the bioavailability of the drug. The easier it is for a particular drug to be metabolized by the liver, lower will be its bioavailability. By definition only when a drug is administered intravenously, is its bioavailability 100% [1]. This factor is kept in mind when designing the dosages for drug via non-intravenous administration. However, though for conventional drugs this may still be an acceptable norm, for hormonal and peptide-based drugs or "protein" drugs, this is no longer feasible as considerable amounts of the drug is lost via the first pass mechanism [2]. Thus, transdermal drug delivery is one of the alternative methods of administering these types of drugs. Transdermal drug delivery is the delivery of drug molecules across the skin barrier layers and into the body. Several methods of transdermal drug delivery have been the focus of active research namely, liquid jet injection, iontophoresis, passive patches, ultrasound, electroporation and microneedles. However, the selected method of microneedles has several clear advantages over other competing methods. One, microneedles are not limited by the size of the drug molecule to be delivered. Two, microneedles are relatively less painful and thus, more patient-friendly to use, resulting in greater patient compliance. Three, depending on their design, the said microneedle system could be produced in a much more low-cost manner. Last but not the least, microneedles could offer the dual flexibility of usage in both drug delivery as well as blood sampling.

The structural material used for the fabrication of microneedles used here is an epoxy-based photopatternable polymer, called SU-8 2050 [from MicroChem Inc, US]. The photopatternability property of SU-8 is exploited here by exposing the SU-8 to UV radiation to cross-link and form the hardened structure resulting in the microneedle body while the rest of the unexposed SU-8 portions are dissolved away. By utilizing this approach, the need for more expensive micofabrication steps such as deep reactive ion etching (DRIE) is eliminated. In conventional microfabrication approaches, DRIE is the more popular technique to create deep trenches inside a solid block of material. Thus, DRIE is replaced by a more elegant lithographic technique instead. This is the underlying principle of the fabrication of the microneedle array utilized here.

Buddhadev P. Chaudhuri is with the Division of Microelectronics and Sensors (MICAS), Dept. of Electrical Engineering (ESAT), Katholieke Universiteit Leuven, Arenberg 10, B-3001 Heverlee, Belgium (phone: +32 16 28 1022, e-mail: buddha@esat.kuleuven.be)

F. Ceyssens is with the Division of Microelectronics and Sensors (MICAS), Dept. of Electrical Engineering (ESAT), Katholieke Universiteit Leuven Arenberg 10, B-3001 Heverlee, Belgium.

C. Van Hoof is with the Interuniversity Microelectronics Center (IMEC), Kapeldreef 75, 3001 Leuven, Belgium and also with the Katholieke Universiteit Leuven, Arenberg 10, B-3001 Heverlee, Belgium.

R. Puers is with the Division Microelectronics and Sensors (MICAS), Dept. of Electrical Engineering (ESAT), Katholieke Universiteit Leuven, Arenberg 10, B-3001 Heverlee, Belgium and also with IMEC, Kapeldreef 75, 3001 Leuven, Belgium.

II. Design

A. Basic mechanical design

From Euler's Column theory [4], we know that the critical failure force, *P*, due to buckling, for a fixed-free column of length *l* is given as:

$$P_{buckling} = \frac{\pi^2 EI}{4l^2} \quad (1)$$

where E is the Young's modulus of elasticity of the material of the microneedle and *I* is the moment of inertia of the microneedle cross-section. *I* about X-X axis through centre of gravity (CG), for a triangular cross-section is given by:

$$I_{tr} = \frac{BH^3}{36} - \frac{bh^3}{36} \quad (2)$$

Fig. 1 illustrates a cross-section of the designed microneedle:

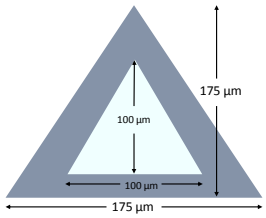

Figure 1: A cross-section of the designed microneedle. Both the triangles are isosceles with each having the height and base as indicated.

With E = 4.02 GPa for the SU-8 used, and the length l being 1000 µm, substituting in (1) and (2), the critical failure force due to buckling, P can be computed to be 230 mN. According to values in literature [5], the skin insertion force of a microneedle of tip diameter less than 15 µm, ranges from 5 mN to 100 mN. Assuming the maximum insertion force of 100 mN, we get:

$$\frac{Failure\ force}{Insertion\ force} > 1 \quad (3)$$

Thus, the microneedle was designed to be mechanically stable during the skin insertion process.

B. Basic geometry and dimensions

A triangular cross-section of the microneedle lumen was selected for the simple reason that the vertex of the triangle aids in enhancing the sharpness of the tip. A schematic diagram of a single hollow microneedle on a platform is as illustrated in Fig. 2.

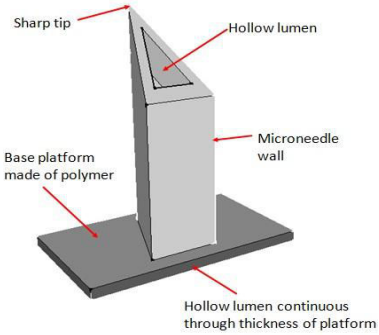

Figure 2. A 3-D representation of the envisaged fabricated single, hollow, triangular cross-section microneedle on a platform.

For intradermal drug delivery, the microneedle design height is around 1000 µm and wall thickness around 30 µm.

III. FABRICATION

The fabrication process as detailed in [3] is fairly straightforward. SU-8 is manually coated on a <100> Si wafer as in Fig. 3. Following the preliminary pre-bakes as described in [3], the SU-8 was exposed to 400 nm wavelength UV at a dosage of 300 mJ/cm^2. Next, a post-exposure bake was performed at 80^{o}C for an hour in an oven. After allowing the substrate to cool down slowly overnight, it was placed in SU-8 developer solution for another hour before the microneedles appear to stand out clearly on the wafer substrate. This is the basic fabrication process.

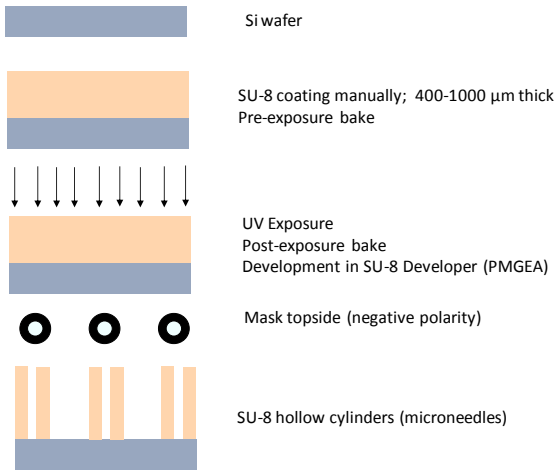

Figure 3. Basic process flow for demonstrating the principle of SU-8 microneedle fabrication. The mask topside shape can be changed as per the desired cross-sectional shape (triangular) of the microneedles.

However, since the hollow lumens of the microneedles are blocked by the wafer substrate itself at the bottom, it would not serve any practical purpose, as passage of fluids is not possible. Thus, a open feedthrough channel is necessary, continuous through the lumen of the microneedle and the thickness of the platform. Additionally, the tips of the microneedles are sharpened by a molding process whereby a <100> Si wafer is anisotropically etched in KOH to create pyramidal pits with its planes inclined at an angle of 54.74^o to the horizontal, and thus to serve as a mold. The microneedles are patterned and molded on these pyramidal pits thus, transferring the angle to the microneedle tips [3]. As can be observed from Fig. 4, the fabrication primarily involves two stages of UV exposure: one for forming the microneedle body and the second one, for forming the platform. The microneedle body is produced by an almost identical process as described in Fig. 2, with the only difference that a 1 mm thick anti-reflection layer of Cr-black is used to prevent undesirable cross-linking of the SU-8 mass during UV exposure, caused by reflection off the inclined planes of the pyramidal pits. The platform layer is produced by a shallow exposure of i-line wavelength of UV at a low dosage of 210 mJ/cm^2 to yield a 200 µm thick platform [6]. Thus, the salient feature of the process is that no additional material is used for making the platform layer and that both the microneedle as well as the platform are made of the same material thus, rendering the process monolithic. Further, alignment of the platform openings with the hollow lumens of the microneedles presents a formidable challenge which has been overcome by providing for a misalignment tolerance of a few microns at the mask design level. After the two levels of UV exposure, the SU-8 is subjected to a post-exposure bake at 80^{o}C for 30 minutes. This is followed by development in PMGEA developer solution for an hour after

which the arrays of microneedles are released automatically from the wafer substrate.

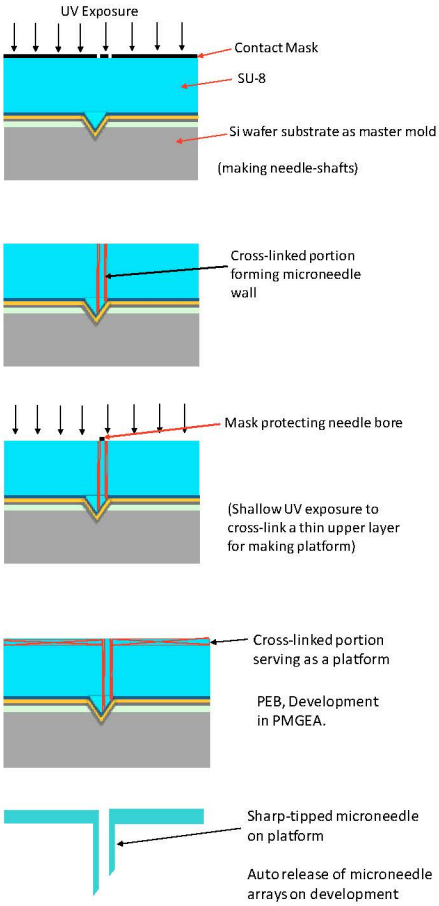

Figure 4. Complete fabrication process yielding hollow sharp-tipped microneedles standing on a platform with its hollow lumen continuous through the needle shaft and platform thickness.

IV. Results

The fabrication results as reported in [3] were still at the preliminary stage. The process described in Fig. 3 was optimized further and the resulting microneedle structures are as depicted in Fig. 5.

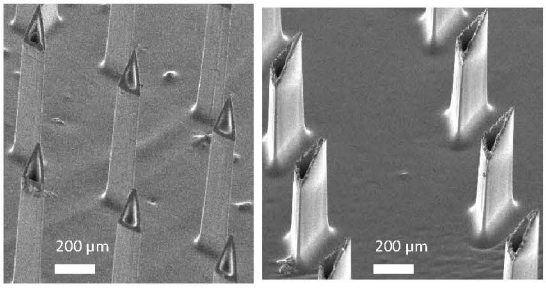

Figure 5. A scanning electron micrograph (SEM) image of the fabricated SU-8 microneedle array of triangular cross-sections with sharp tips, standing out-of-plane on the SU-8 platform with the hollow lumens continuous through the platform thickness. *Dimensions:* Microneedle height = 1000 µm, average wall thickness = 25 µm, Platform thickness = 200 µm. *(Left)* The needle bores are closed due to an incomplete development. *(Right)* The needle bores are seen to be clearly open.

Thus, the above Fig. 5 demonstrates that triangular cross-section microneedles with sharp tips and hollow lumens were successfully fabricated with the given process. Further, the measured height of 1000 µm with an average wall thickness of 25 µm indicates that a high aspect ratio of 40 has been achieved, which is novel considering the hollow nature of the lumens in the out-of-plane structures, and no use of DRIE. A close-up view of the sharp tips in Fig. 5 further proves that the tip sharpening by molding has been successful.

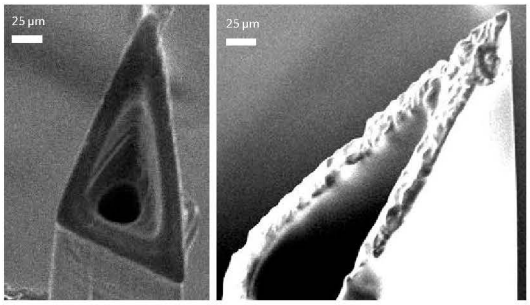

Figure 6. An SEM image of the close-up of fabricated microneedle tips. *(Left)* Tip diameter measuring approximately around 8 µm. *(Right)* Tip diameter measuring approximately less than 5 µm.

V. Mechanical Tests

The fabricated microneedle arrays were subjected to compressive mechanical testing to determine the critical failure load. This is for ascertaining the maximum force that can be withstood by the microneedles during skin puncturing. For this purpose, a microneedle array comprising 45 needles was loaded with a plumber on its sharp-tipped ends, applying uniform load increasing incrementally, on the entire needle array. The load-displacement graph given in Fig. 7 shows that the peak load applied is 10.35 N on the 45 needles after which the graph undergoes an explicit drop indicating an avalanche of failures of the needles. However, on closer inspection, it can be observed that the first failure already occurs at the 7.8 N mark. Thus, on taking 7.8 N as the minimum critical force, the average critical failure load may be said to be around 173 mN per microneedle in contrast to the 230 mN designed critical load. If skin insertion force ranges around 100 mN [5], the computed safety factor of 1.73 is still greater than 1, and thus, should be sufficient.

VI. Discussion & Conclusion

High aspect ratio, out-of-plane, hollow, sharp-tipped microneedles-on-a-platform were fabricated using an elegant, repeatable process with a low-cost, monolithic approach. Mechanical tests results were encouraging, indicating that the microneedles should be strong enough for skin penetration without failure. Though several research groups have been working on fabrication of polymer microneedles, the work presented here is quite novel in terms of the geometrical cross-section of the microneedles, the high-aspect-ratios

achieved, the use of the Cr-black anti-reflection layer as well as the auto release of the microneedles from the wafer

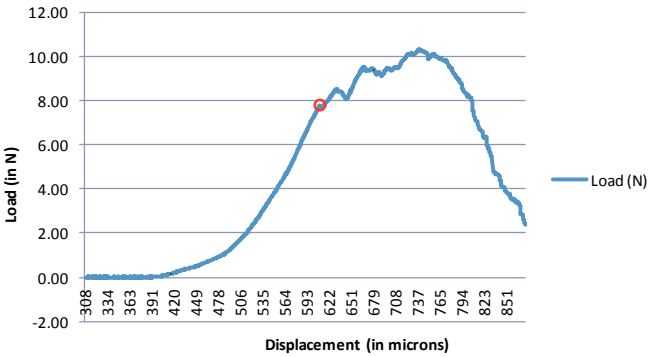

Figure 7. Load-displacement graph to determine failure load of the fabricated microneedles. Though peak applied load is 10.35 N, the first failure occurs at 7.8 N (circled in red), resulting in an average failure load of 173 mN per microneedle.

substrate without the need for a sacrificial layer. Wang et al [7] used a similar molding-cum-double layer exposure approach but employed PDMS molds instead, thereby limiting the attainable aspect ratios and the sharpness of tips. They achieved tip diameters of around 15 µm and an aspect ratio of about 16.

Future work includes further optimizing the fabrication process and mechanical tests of real skin penetration followed by microfluidic characterization and biological tests of the microneedles.

VII. Acknowledgment

The authors wish to acknowledge the role of Interuniversity Microelectronics Centre (IMEC), Belgium for funding this work as part of a PhD research. Further continuation of this work has been made possible by a research grant from the Flemish Government's IWT agency, and the authors are grateful for this.

References

[1] R. Nassiri, "Introduction to Pharmacology," *Michigan State University,* Medical Mission Trip, Dominican Republic.

[2] Taki Y, Sakane T, Nadai T, Sezaki H, Amidon GL, Langguth P, Yamashita S., "First-pass metabolism of peptide drugs in rat perfused liver," 9, Sep 1998, *J Pharm Pharmacol.,* Vol. 50, pp. 1013-8.

[3] B. P. Chaudhri et al, "Out-of-Plane, High strength, Polymer Microneedles for Transdermal Drug Delivery," *33rd Ann. Int. Conf. IEEE EMBS*, Boston, Aug. 2011, proc., pp. 3680-3683.

[4] S. Timoshenko, *Theory of Elastic Stability* New York, McGraw-Hill, 1961.

[5] S.P. Davis, B.J. Landis, Z.H. Adams, M.G. Allen, M.R. Prausnitz, "Insertion of microneedles into skin: measurement and prediction of insertion force and needle fracture force," 2004, *J. Biomech*, Vol. 37, pp. 1155-1163.

[6] F. Ceyssens, R. Puers, *J. of Micromech. Microeng*., 16, 2006, pp. S19-S23.

[7] P-C Wang, B. A. Wester, S. Rajaraman, S-J Paik, S-H Kim, and M. G. Allen, "Hollow Polymer Microneedle Array Fabricated by Photolithography Process Combined with Micromolding Technique," *31st Ann. Int. Conf. IEEE EMBS,* Minneapolis, Minnesota, USA, Sept. 2009.